nature biotechnology

Production of pancreatic hormone–expressing endocrine cells from human embryonic stem cells

Kevin A D'Amour, Anne G Bang, Susan Eliazer, Olivia G Kelly, Alan D Agulnick, Nora G Smart, Mark A Moorman, Evert Kroon, Melissa K Carpenter & Emmanuel E Baetge

Of paramount importance for the development of cell therapies to treat diabetes is the production of sufficient numbers of pancreatic endocrine cells that function similarly to primary islets. We have developed a differentiation process that converts human embryonic stem (hES) cells to endocrine cells capable of synthesizing the pancreatic hormones insulin, glucagon, somatostatin, pancreatic polypeptide and ghrelin. This process mimics *in vivo* pancreatic organogenesis by directing cells through stages resembling definitive endoderm, gut-tube endoderm, pancreatic endoderm and endocrine precursor—en route to cells that express endocrine hormones. The hES cell–derived insulin-expressing cells have an insulin content approaching that of adult islets. Similar to fetal β-cells, they release C-peptide in response to multiple secretory stimuli, but only minimally to glucose. Production of these hES cell–derived endocrine cells may represent a critical step in the development of a renewable source of cells for diabetes cell therapy.

The shortage of transplantable pancreatic islets to treat diabetes has stimulated much research focused on generating renewable sources of insulin-producing β-cells. Human embryonic stem (hES) cells have a virtually unlimited replicative capacity and the potential to produce most, if not all, differentiated cell types[1,2]. Many studies have reported the differentiation of insulin-producing cells from mouse ES cells and, more recently, from human ES cells[3–9]. However, these methods have various limitations, including inefficiency of differentiation, low insulin content of the insulin-producing cells, a reliance on non-directed ES cell differentiation, generation of insulin-producing neural cell lineages[10–12], a lack of evidence that the insulin-producing cells are derived from the endoderm lineage, and uptake of exogenous insulin from the medium[12–14]. These issues suggest that producing functional β-cells from ES cells is not straightforward. A more plausible approach may be to direct ES cells through a process that mimics normal pancreatic development.

The pancreas develops from the definitive endoderm (DE) germ layer, which is generated during the gastrulation stage of embryogenesis in an area termed the primitive streak[15]. DE initially consists of a flat sheet of cells that has anterior-posterior pattern information. This flat sheet then forms a primitive gut tube, along which the domains for various endoderm organ primordia are specified[16]. The pancreas develops from the posterior foregut, emerging as buds from the dorsal and ventral sides of the gut tube. At this early stage, formation of the pancreatic anlage depends on retinoid signaling and on inhibition of hedgehog signaling[17,18]. The developing organ is composed of *Ipf1* (also known as *Pdx1*)-expressing epithelial progenitors that will give rise to the endocrine, exocrine and ductal cells of the pancreas[19]. This epithelium also expresses the transcription factor genes *Hlxb9*, *Hnf6* (also known as *Onecut*), *Ptf1a* and *Nkx6-1*, which, together with *Pdx1*, encode proteins that are important in pancreatic development[20]. After initial bud formation, further growth, branching and differentiation of the pancreatic epithelium depends on signals from the adjacent mesenchyme, such as mesenchymal Fgf10 (ref. 21).

The next phase of pancreas development is endocrine cell specification, which occurs through inhibition of Notch signaling in some cells of the pancreatic epithelium, allowing expression of the pro-endocrine gene *Neurog3* (also called *Ngn3*)[20]. *Ngn3* is expressed in all endocrine progenitors[19], initiating a cascade of transcription-factor expression that controls endocrine cell differentiation. The critical transcription factor genes include *Nkx2-2*, *Neurod1*, *Nkx6-1*, *Pax4*, *Pax6* and *Isl1*. During this period, the nascent endocrine cells migrate from the branched epithelium into the surrounding mesenchyme to form the islets of Langerhans. Islets comprise five endocrine cell types: α, β, δ, PP and ε cells, which produce the hormones glucagon, insulin, somatostatin, pancreatic polypeptide and ghrelin, encoded by *Gcg*, *Ins*, *Sst*, *Ppy* and *Ghrl*, respectively. The mechanisms that control the specification of these endocrine cell types from *Ngn3*-expressing progenitors are not well understood. Once formed, the hormone-expressing endocrine cells undergo further differentiation to a mature functional state, which, for a β-cell, involves the ability to release insulin in response to elevated glucose.

Learning how to direct hES cells *in vitro* through progressive stages of commitment to cells resembling β-cells presents substantial challenges. Although there is a considerable body of literature devoted to pancreatic organogenesis that can guide differentiation strategies, some aspects of pancreatic development remain poorly understood[16,20,22,23]. Also, cells *in vitro* are unlikely to behave exactly like cells in the intricate

Novocell Inc., 3550 General Atomics Ct., San Diego, California 92121, USA. Correspondence should be addressed to E.E.B. (ebaetge@novocell.com).

Received 31 August; accepted 3 October; published online 19 October 2006; doi: 10.1038/nbt1259

context of an embryo. Therefore, our strategy combines an informed approach based on developmental biology and an empirical approach.

Previously we described a method for differentiating hES cells to DE[24]. Here we show that DE derived from hES cells can be efficiently differentiated to hormone-expressing endocrine cells through a series of endoderm intermediates similar to those that occur during pancreatic development. The insulin content of the insulin-expressing cells approaches that of adult islets. In addition, C-peptide release occurs in response to multiple secretory stimuli, although only minimally to glucose, similar to what occurs in the fetal β-cell.

RESULTS

Directed pancreatic differentiation of hES cells

We have developed a five-step protocol for differentiation of hES cells to pancreatic hormone–expressing cells (**Fig. 1a** and Methods). The protocol was optimized primarily in the CyT203 cell line in a stepwise fashion. We focused first on generating DE, followed by *PDX1*-expressing cells and, finally, insulin-expressing cells. Study of the developmental biology literature led us to test the action of such factors as activins, Wnt3a, BMPs, TGFβ1, TGFβ inhibitors, FGFs, FGF inhibitors, retinoids, γ-secretase inhibitors, GLPs and analogs, HGF, IGFs, VEGF, nicotinamide and hedgehog inhibitors. The empirical approach involved testing various concentrations, times of administration, lengths of application and combinations of factors as well as assorted medium formulations in which the factors were applied. The effects of various treatments on differentiation were initially evaluated using real-time PCR to detect expression of 30 or more markers of both target and non-target cell types monitored at short intervals throughout the course of differentiation. After initial optimization of the protocol, the differentiation process was also characterized at the level of protein expression by immunofluorescence, western blotting, flow cytometry and ELISA.

In stage 1, hES cells are transitioned through mesendoderm to DE using high concentrations of activin A (100 ng/ml) in the context of low FBS supplementation, as previously reported[24]. We subsequently improved this procedure by shortening the activin A treatment period to 3 d and adding Wnt3a during the first day of activin exposure[25]. These modifications increased the efficiency of mesendoderm specification and the synchrony of DE formation (data not shown). As with the protocol of ref. 24, the hES cell–derived DE expressed the DE markers *SOX17* (ref. 26) and *CXCR4* (refs. 24,27,28), and showed anterior character as indicated by expression of the anterior DE markers *CER* and *FOXA2* (refs. 29,30; **Figs. 1b** and **2a–c**; **Supplementary Figs. 1** and **2a** online).

We found that initial specification of hES cells to DE is critical for efficient production of pancreatic hormone–expressing cells. If the activin A dose was lowered, thereby altering the quantity and anterior pattern of the DE produced, differentiation to endoderm intermediates and endocrine cells was considerably reduced (**Supplementary Fig. 1** online). Moreover, if neural or extraembryonic lineages were specified from hES cells, these populations failed to differentiate to endocrine cells or their endoderm precursors (**Supplementary Fig. 2a**,**b** online).

In stage 2, activin A is removed, which in our cultures seems to be essential to allow the transition of DE to a stage resembling the primitive gut tube. In the mouse embryo, at embryonic day 8 (E8), the transcription factor *Tcf2* (also called *Hnf1b*) is expressed in the entire primitive gut tube[31,32]. Approximately 12 h later *Hnf4a* shows a similar pattern of expression[33]. In zebrafish, *hnf1b* is involved in patterning the posterior

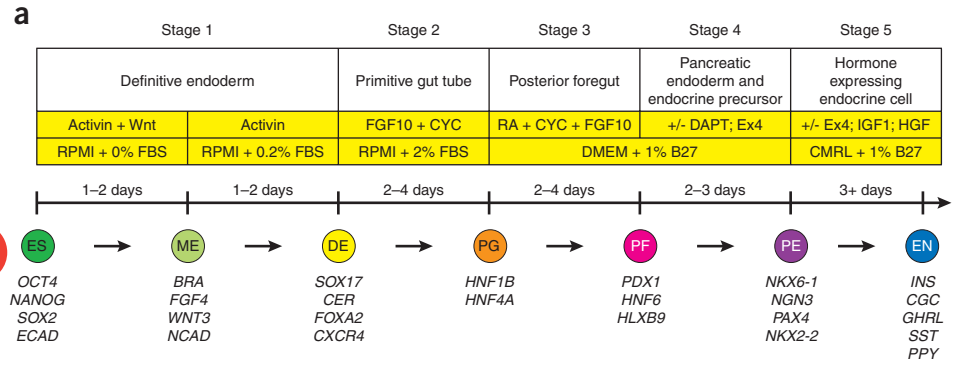

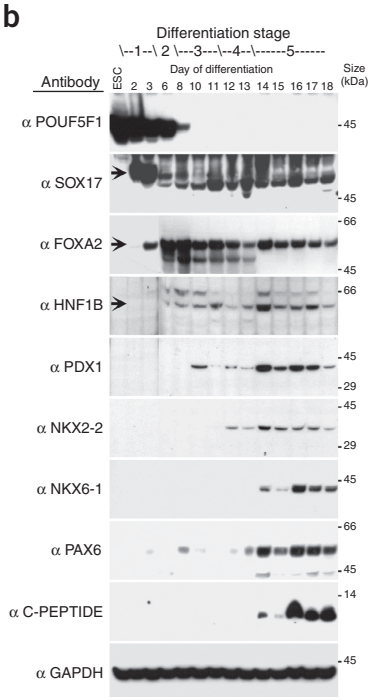

Figure 1 Schematic of differentiation procedure and protein expression for some key markers of pancreatic differentiation. (**a**) The differentiation protocol is divided into five stages and the growth factors, medium and range of duration for each stage are shown. This protocol orchestrates differentiation through five identifiable endodermal intermediates en route to production of hormone-expressing endocrine cells. Several markers characteristic of each cell population are listed. CYC, KAAD-cyclopamine; RA, all-*trans* retinoic acid; DAPT, γ-secretase inhibitor; Ex4, exendin-4; ES, hES cell; ME, mesendoderm; DE, definitive endoderm; PG, primitive gut tube; PF, posterior foregut endoderm; PE, pancreatic endoderm and endocrine precursor; EN, hormone-expressing endocrine cells. (**b**) Western blot analyses show the dynamics of protein expression for several key markers of pancreatic differentiation. α, antibody. POU5F1 (OCT4): this marker of undifferentiated ES cells gradually diminishes as cells differentiate and becomes undetectable during stage 3. SOX17: the highest levels of the full-length SOX17 protein (arrow) are observed during differentiation of definitive endoderm (stage 1). At later stages it gradually diminishes, while a slightly faster-migrating protein accumulates. This corresponds to the truncated form of SOX17 (ref. 70), and its presence throughout later stages of differentiation is consistent with the continued expression of SOX17 mRNA (**Supplementary Fig. 2a**). See ref. 24 for a demonstration of SOX17 antibody specificity. FOXA2: the upper band (arrow) seen at all stages from the end of stage 1 onward corresponds to the 48-kDa FOXA2 protein. We believe that partial degradation results in the faster-migrating band seen in some samples. HNF1B: the lower band (arrow) seen from stage 2 onward corresponds to the 61-kDa variant of the HNF1B protein. We do not currently know the source of the slower-migrating band seen in some samples. PDX1: this accumulates during stage 3 and diminishes at the end of stage 5. NKX2-2: is present during stages 4 and 5. NKX6-1: this is detectable at the end of stage 4 and in stage 5. PAX6: this is most strongly expressed during stage 5. C-peptide: although this antiserum is immunoreactive with both the fully processed C-peptide and the unprocessed proinsulin, the size of the band is most consistent with the 9-kDa proinsulin. C-peptide + proinsulin accumulate during stage 5.

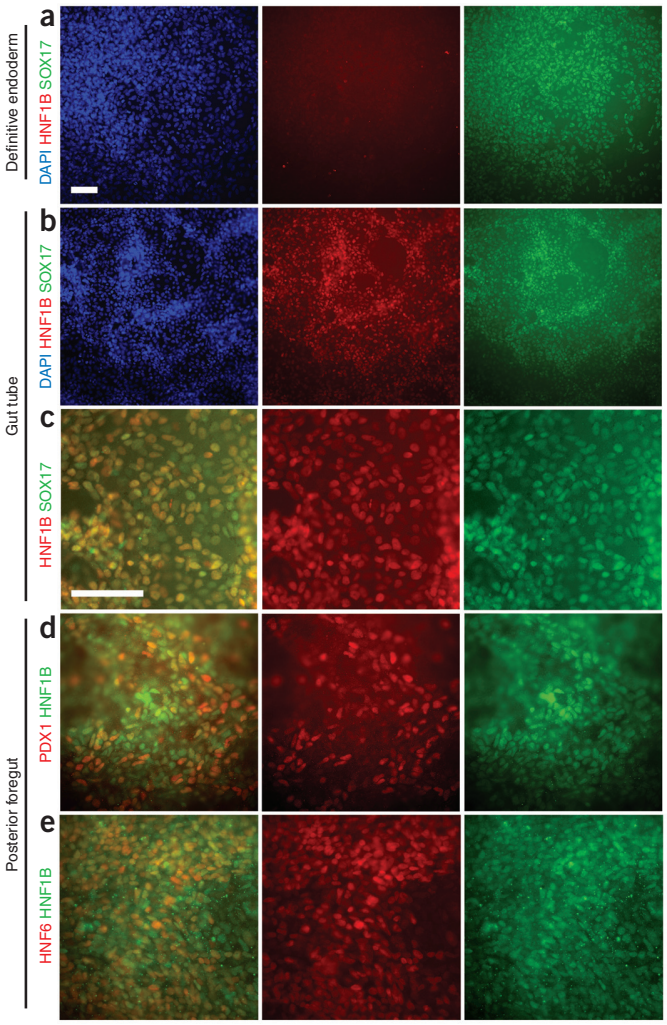

Figure 2 Immunofluorescence analysis of transitions from definitive endoderm to gut tube and from gut tube to posterior foregut. (**a**–**e**) Fluorescence micrographs showing marker expression at the definitive endoderm (**a**), gut-tube endoderm (**b**,**c**) and posterior foregut endoderm (**d**,**e**) stages. Each micrograph is uncoupled into blue (DAPI; left), red (middle) and green channels (right). (**a**) HNF1B-expressing cells (red) are not detected at the DE stage, whereas SOX17-expressing cells (green) are abundant in the culture. (**b**) At the gut-tube endoderm stage, most SOX17-expressing cells (green) coexpress HNF1B (red). (**c**) Higher magnification of **b** showing coexpression of HNF1B (red) and SOX17 (green). (**d**) At the posterior foregut stage, PDX1 (red) is induced in a subset of HNF1B-expressing cells (green). (**e**) At the posterior foregut stage, HNF6 (red) is induced in a subset of HNF1B-expressing cells (green). Scale bars, 100 μm.

region of the foregut[34]. During stage 2, we observed a considerable upregulation of the gut-tube markers *HNF1B* and *HNF4A* at both the mRNA and protein levels (**Figs. 1b** and **2**; **Supplementary Figs. 1** and **2a** online). Simultaneously, expression of the DE markers *CER* and *CXCR4* was considerably reduced (**Supplementary Figs. 1** and **2a** online). Notably, *SOX17* continued to be expressed in the HNF1B-positive cells, demonstrating their endodermal origin (**Fig. 2b**,**c**). Although removal of activin A was sufficient to induce expression of gut-tube markers, addition of FGF10 and the hedgehog-signaling inhibitor KAAD-cyclopamine provided further benefit, as evidenced by increased expression of *INS* mRNA during stage 5 of differentiation. Addition of FGF10 and KAAD-cyclopamine resulted in a 160-fold increase in *INS* mRNA compared with activin removal alone (data not shown).

In stage 3, the gut-tube endoderm is exposed to retinoic acid (RA) together with KAAD-cyclopamine and FGF10. Upon addition of RA, the cells rapidly began to express high levels of *PDX1* and *HNF6* while maintaining or increasing expression of *HNF1B* and *HNF4A* (**Figs. 1b** and **2d**,**e**; **Supplementary Figs. 1** and **2b** online). Expression of this combination of genes is indicative of posterior foregut. Interestingly, if RA is not added at the gut-tube endoderm stage, no appreciable *NGN3*, *INS* or *GCG* gene expression is observed at later stages, despite the appearance of *PDX1* expression (data not shown). This is consistent with studies in several model systems that demonstrate the necessity of retinoid signaling for pancreatic development[35–38]. In addition, if KAAD-cyclopamine is omitted at this stage, the levels of *INS* mRNA observed at stage 5 are lower (data not shown). This result is in agreement with studies in mice that show a requirement for low hedgehog signaling during pancreatic bud specification[39].

During stage 4, the *PDX1*-expressing posterior foregut endoderm cells are recruited to the pancreatic and endocrine lineages. We observed extensive regions of cells coexpressing PDX1 and NKX6-1 or HNF6 and NKX6-1 across the culture dish, characteristic of pancreatic epithelium (**Fig. 3a** and data not shown). NKX2-2–expressing cells were found scattered within and at the periphery of regions of PDX1 and NKX6-1–expressing pancreatic epithelium; the majority of the NKX2-2 cells coexpressed PDX1 and more rarely NKX6-1 (**Fig. 3b–e**), which identifies them as being derived from pancreas, anterior stomach or duodenum. In addition, many NKX2-2 cells coexpressed NGN3, reflecting initial commitment to the endocrine lineage. Consistent with the process of endocrine precursor specification in mouse[20], we observed transient expression of *NGN3* and *PAX4* in addition to sustained expression of *NKX2-2* as the endocrine precursors emerged (**Figs. 3b–d**; **Supplementary Figs. 1** and **2b** online).

During stage 5, by about 15 d of differentiation, endocrine cells expressing the pancreatic hormones insulin, glucagon, somatostatin, pancreatic polypeptide and ghrelin are produced (**Figs. 1b**, **3e**,**f** and **4**; **Supplementary Figs. 1** and **2b** online). As determined by immunofluorescence, the endocrine cells coexpressed the pan-endocrine markers NEUROD1, ISL1, PAX6 and synaptophysin (encoded by *SYP*), and cells that expressed insulin also expressed islet amyloid polypeptide (encoded by *IAPP*) (**Figs. 3f** and **4** and data not shown). Moreover, the insulin-expressing cells coexpressed PDX1 and NKX2-2 (**Fig. 3e**). We note that hormone expression initially did not appear to fill the cytoplasm (**Fig. 3e**), whereas at later stages hormones filled and delineated the cytoplasm (**Figs. 3f** and **4**). A proportion of the endocrine cells coexpressed insulin and glucagon or insulin and somatostatin, and rare cells expressed all three hormones. Pancreatic polypeptide was also coexpressed with insulin, glucagon or somatostatin. In contrast to the other endocrine hormones, ghrelin, with rare exceptions, was not coexpressed with other hormones (**Fig. 4a**,**b** and data not shown). To analyze coexpression, we specifically imaged areas of the culture where endocrine cells were present primarily in monolayers; however, many of the endocrine cells were in multilayered regions and intermingled with PDX1 and NKX6-1–expressing pancreatic epithelium.

To quantify the numbers of insulin-expressing cells present during stage 5, we differentiated hES cells using either 30 or 100 ng/ml of activin A for the first 3 d to generate cultures with different proportions of insulin-positive cells. These two conditions produced cultures that varied by >200-fold in insulin mRNA levels (data not shown; see also **Supplementary Fig. 1** online) and showed obvious differences in the number of insulin-immunoreactive cells (**Fig. 5a**). Consistent with these data, analysis by flow cytometry showed that cultures treated with the high dose of activin A (100 ng/ml) yielded 7.3% insulin-positive cells

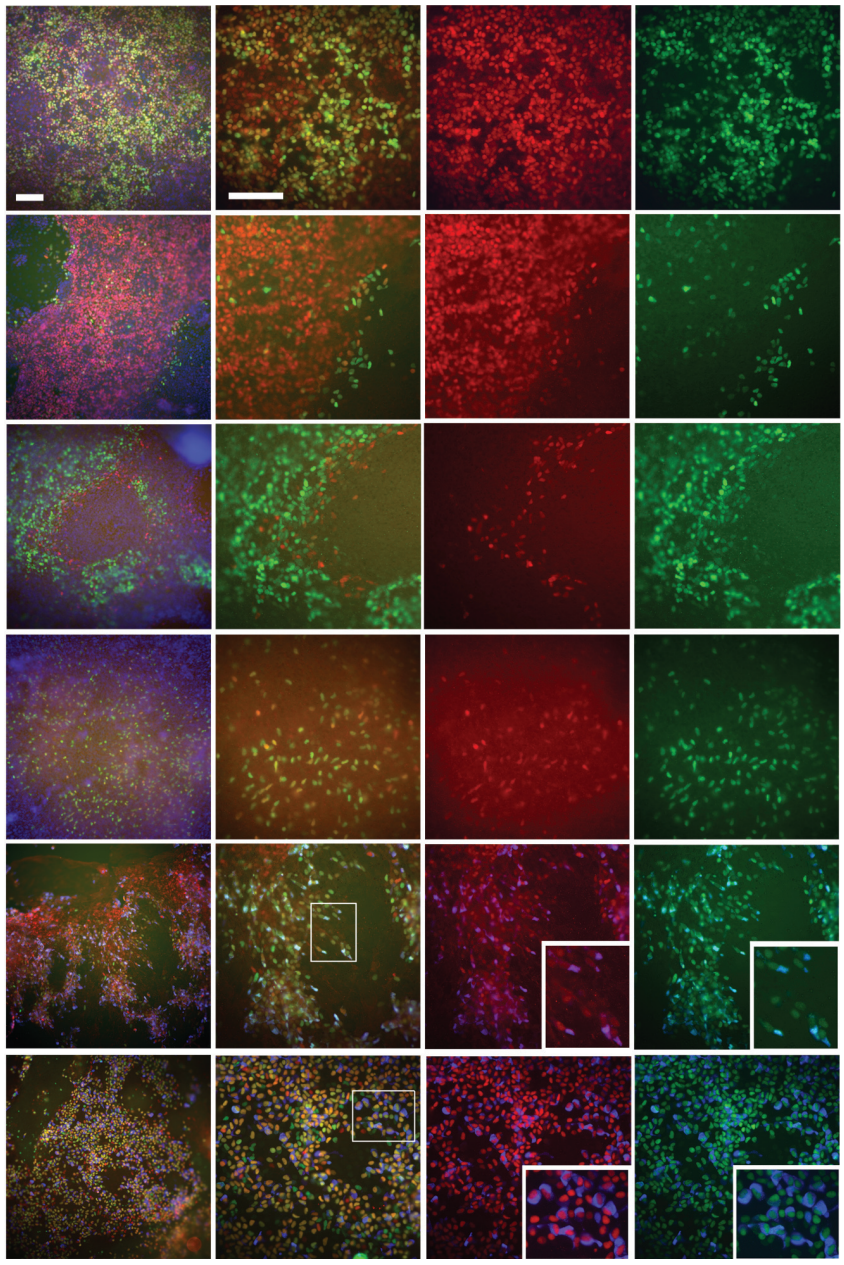

Figure 3 Immunofluorescence analysis of transitions from pancreas to endocrine precursor and from endocrine precursor to hormone-expressing cells. (**a**–**f**) Fluorescence micrographs showing expression of the indicated marker genes at the endocrine precursor (**a**–**d**) and hormone-expressing (**e**,**f**) stages. In each row, the first panel shows a low-magnification view of merged blue, red and green channels, and a higher-magnification view of the same field is shown in the next three panels. (**a**,**b**) Extensive regions of cells in the culture dish express PDX1 (red) at the endocrine precursor stage; note that the DAPI staining in the first panels of each row indicates regions that are clearly positive and negative for PDX1 expression. Many PDX1-expressing cells (red) coexpress NKX6-1 (green), which is characteristic of pancreatic epithelium (**a**). The onset of NKX2-2 (green) expression occurs in a subset of cells that emerge from the PDX1 (red) domains (**b**). Many NKX2-2 positive cells are also PDX1 positive, although some express PDX1 less intensely than others. Some NKX2-2–expressing cells are PDX1 negative. Frequently, the NKX2-2 cells emerge from the edges of the PDX1 domains. (**c**) NKX2-2–expressing cells (red) emerge from NKX6-1–positive domains (green). A small number of NKX2-2–expressing cells are copositive for NKX6-1, although the majority of these express NKX6-1 only weakly. (**d**) NGN3-expressing cells (red) appear transiently in the cultures and many are copositive for NKX2-2 (green). (**e**) Nascent insulin-expressing cells (blue) coexpress PDX1 (red) and NKX2-2 (green). Insets, higher magnifications of nascent insulin-expressing cells that coexpress PDX1 and NKX2-2; note that these cells express lower levels of insulin, which does not appear to fill the cytoplasm. (**f**) Insulin-expressing cells (blue), as well as other endocrine cells in the field, coexpress PAX6 (red) and ISL1 (green). Insets, higher magnifications of PAX6- and ISL1-positive insulin-expressing cells; in contrast to what is seen in **e**, the hormone expression fills and delineates the cytoplasm of these later-stage cells, which have been cultured 4 d longer than those in **e**. Scale bars, 100 μm.

at day 16 of differentiation, whereas the low dose (30 ng/ml) resulted in only 0.3% insulin-positive cells. As expected, all the insulin-positive cells coexpressed synaptophysin[40,41]. To date we have generated cell populations in which as many as 12% of the cells are insulin positive and 20.7% of the cells express the pan-endocrine marker synaptophysin (**Fig. 5b**). The average percentage of insulin-positive cells in differentiated hES cell cultures was 7.3% (n = 11, range 3–12.0%) and the average percentage of synaptophysin-positive cells was 13.4% (n = 6, range 10–20.7%).

We also compared mRNA levels of several markers during the five stages of differentiation to those of human fetal and adult pancreas (**Supplementary Fig. 3** online). The expression levels of *PDX1*, *NGN3*, *INS* and *GCG* were equivalent to those observed at various stages of human pancreas development. The levels of *SST* and *GHRL* were greater than those observed in adult pancreas, but lower than the peak levels observed during human fetal pancreatic development.

In addition to pancreatic endocrine cells, amylase-expressing exocrine cells were found in areas of pancreatic epithelium and endocrine cell differentiation (**Supplementary Fig. 4** online). Taken together, these data suggest that we have generated cell populations with pancreatic identity from hES cells.

hES cell–derived endocrine cells have a high insulin content

Regions of pancreatic endocrine cells in the cultures could be specifically labeled with the zinc-chelating dye dithizone (DTZ), which efficiently stains β-cells in the islet owing to the presence of zinc in insulin-containing secretory granules[42]. We observed discrete areas of DTZ staining in stage 5 cultures (**Supplementary Fig. 5a–d** online). As this dye can also stain non-pancreatic zinc-containing cells[43], we selected the DTZ-stained areas of the culture and compared their gene expression to that of the whole population. The DTZ-stained areas were highly enriched for expression of pancreatic hormones and *PDX1* (**Supplementary**

Fig. 5e–i online) and were depleted in expression of markers of DE, neural and mesoderm lineages (**Supplementary Fig. 5j–l** online).

Next, we compared the insulin content of hES cell–derived cells and primary adult human islets. Western blot analyses indicated that whereas both contained comparable amounts of C-peptide, which is processed from proinsulin, only hES cell–derived cells contained large amounts of proinsulin (data not shown). To more accurately quantify these observations, we measured both C-peptide and proinsulin by ELISA and combined the results to arrive at a value for total insulin content in DTZ-stained hES cell–derived cells and adult human islets (**Fig. 6a**). The total insulin content was similar, as evidenced by the overlapping range of values obtained for each. The average proportion of total insulin content attributable to C-peptide in hES cell–derived cells and human islets was 64% (range 49–90%) and 97% (range 92–99%), respectively, consistent with a lower level of proinsulin processing in hES cell–derived cells.

Insulin release from hES cell–derived endocrine cells

To confirm the *de novo* synthesis and release of insulin by hES cell–derived insulin-expressing cells[13], we monitored the release of C-peptide into the culture medium in response to various stimuli (**Fig. 6b**). Direct depolarization of the cells by addition of potassium chloride (KCl) consistently resulted in two- to sixfold increases in secreted C-peptide during 1-h incubations. We inferred the presence of functional ATP-sensitive potassium (K_{ATP}) channels in the cells from three- to sevenfold increases in C-peptide release over basal levels upon the addition of tolbutamide, an inhibitor of K_{ATP}-channels[44]. The presence of K_{ATP} channels was also indicated by expression of mRNA for the subunits *ABCC8* (*SUR1*) and *KCNJ11* (*KIR6-2*) (data not shown). Treatment with the L-type voltage-dependent calcium channel (VDCC) agonist (–)-BAY K8644 resulted in a small but consistent stimulation of C-peptide release, suggesting activation of VDCCs[45]. We also evaluated the cells' responsiveness to cAMP, which influences insulin secretion in several ways[46,47]. We observed robust increases in C-peptide secretion when the levels of cAMP were increased by treatment with the phosphodiesterase inhibitor 3-isobutyl-1-methylxanthine (IBMX). Studies of nutrient secretagogues showed that addition of methylpyruvate increased C-peptide release three- to sevenfold over basal levels. Stimulation either with α-ketoisocaproic acid (KIC) or with L-leucine and L-glutamine increased C-peptide release by about twofold. With the exception of L-leucine plus L-glutamine, C-peptide release induced by these stimuli was observed in every case tested (N = 3–15 experiments). In contrast, release induced by D-glucose was observed in one out of ten instances (N = ~50 experiments) at 30–300% induction over basal glucose conditions (data not shown). However, glucose-induced C-peptide release was a consistent finding with adult islets (**Fig. 6b**).

When the cells were depolarized by addition of KCl, C-peptide release into the medium was extremely rapid (**Fig. 6c**), increasing fivefold above basal levels within 4 min. The response to methylpyruvate was slower, with C-peptide levels surpassing basal levels by 8–12 min (**Fig. 6d**). The rapid kinetics of C-peptide release indicates that the insulin-expressing cells have a pool of vesicles that are ready to be secreted in response to appropriate stimuli.

Consistent with the rapid insulin release kinetics, we observed that hES cell–derived endocrine cells contained numerous secretory granules (**Fig. 6e** and **Supplementary Fig. 6** online). Multiple endocrine cells were imaged, and although most cells showed a mixture of granule morphologies, several contained granules with a clear halo surrounding the dense core, a morphology characteristic of insulin-containing granules[48].

Multiple hES cell lines produce endocrine cells

All the data presented thus far were generated using the CyT203 cell line. We applied our differentiation procedure to five additional hES cell lines (CyT25, CyT49, BG01, BG02 and BG03) and in all cases produced endocrine cells, albeit at different efficiencies. All hES cell lines examined transitioned through the same developmentally appropriate intermediates and produced insulin-expressing cells, as demonstrated by real-time PCR (**Supplementary Fig. 7** online and data not shown). For several of the cell lines, we showed that the insulin-expressing cells stained with DTZ, had similarly high C-peptide content and responded to the same secretory stimuli (**Supplementary Fig. 7** online). The lower efficiency of endocrine differentiation observed for some cell lines was not unexpected, as we optimized the differentiation procedure primarily using the CyT203 line. In some lines, a deficit occurs before the production of *PDX1*-expressing endoderm at stage 3 (BG01 and BG02).

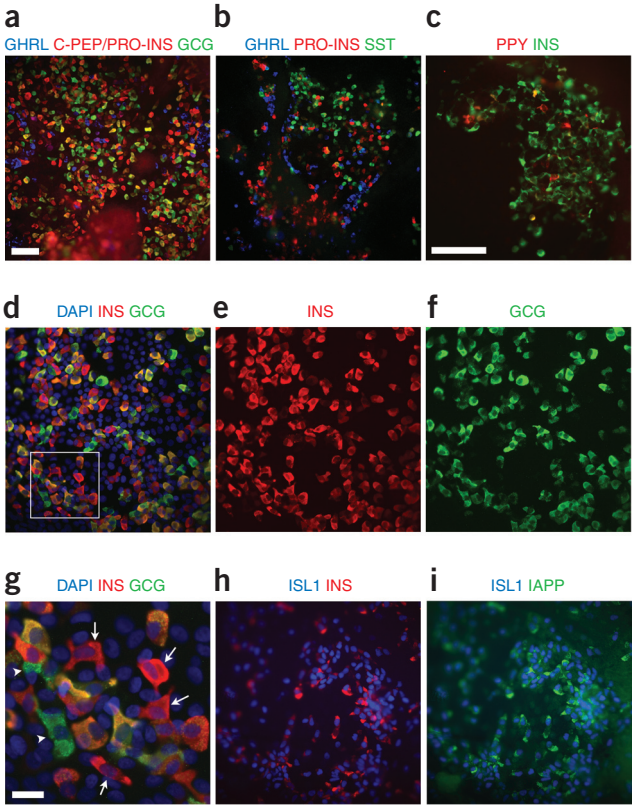

Figure 4 Immunofluorescence analysis of hormone-expressing cells. (**a**) Triple staining showing that ghrelin-expressing cells (blue) do not coexpress either proinsulin or C-peptide (red) or glucagon (green), but that in some cells proinsulin or C-peptide and glucagon are coexpressed. (**b**) Triple staining showing that ghrelin-expressing cells (blue) do not coexpress proinsulin (red) and somatostatin (green) but that in some cells proinsulin and somatostatin are coexpressed. (**c**) A relatively small number of PPY-expressing cells (red) are observed compared with the number of insulin (green) cells; some PPY-expressing cells coexpress insulin. (**d**–**f**) A higher-magnification view comparing merged and uncoupled fluorescence micrographs of endocrine cells expressing insulin (red) and glucagon (green) showing that some cells express both hormones whereas others express only one. Note the DAPI staining in **d** shows that this field of cells is primarily a monolayer, allowing assessment of copositivity for insulin and glucagon. (**g**) A higher-magnification view of the boxed area in **d** showing several cells expressing insulin but not glucagon (arrows) and glucagon but not insulin (arrowheads). (**h**–**i**) Triple staining uncoupled into two fluorescence micrographs showing coexpression of insulin (red) and IAAP (green) in many ISL1-expressing endocrine cells (blue). Scale bars, 100 μm (**a**) and (**c**), 20 μm (**g**).

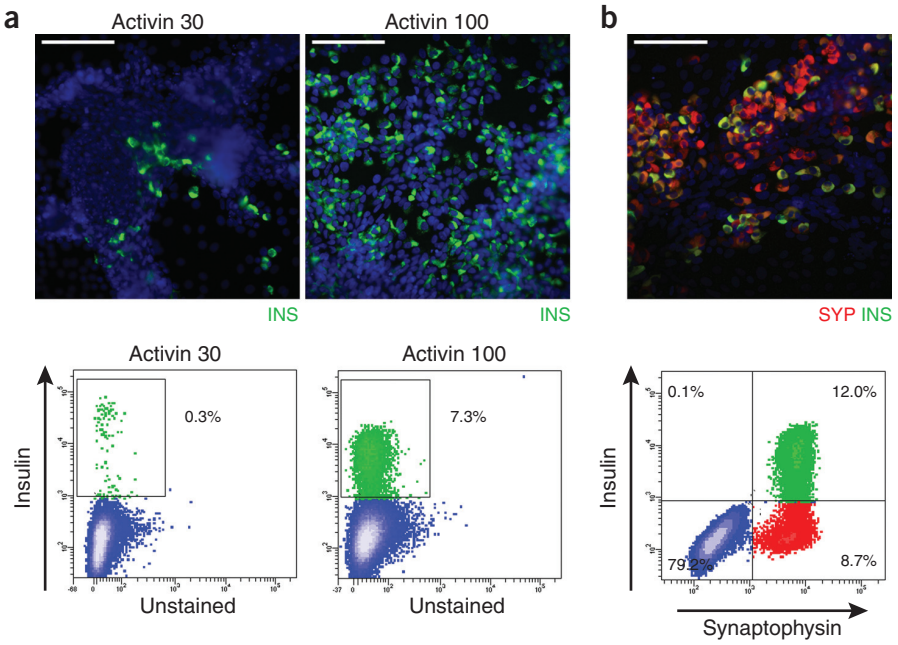

Figure 5 Flow cytometry analysis of insulin-expressing cells. (**a**) Human ES cell cultures were differentiated for 3 d in activin A at either 30 ng/ml or 100 ng/ml followed by equivalent treatment through the remainder of the differentiation stages. As demonstrated by both immunofluorescence (top) and flow cytometry analysis (bottom), treatment with 30 ng/ml activin A produces fewer insulin-expressing cells (0.3%) than treatment with 100 ng/ml activin A (7.3%). (**b**) Differentiating human ES cell cultures contain cells that immunostain for both insulin (green) and synaptophysin (red) as determined by immunofluorescence (top). DAPI (blue) labels cell nuclei. Flow cytometry analysis (bottom) showed that the cultures can comprise 20.7% synaptophysin-expressing cells and 12.0% insulin- and synaptophysin-coexpressing cells. Scale bar, 100 μM.

DISCUSSION

We have described a five-stage protocol for efficiently differentiating hES cells to endocrine hormone–expressing cells through a series of endodermal intermediates resembling those that occur during pancreatic development *in vivo*. We characterized the differentiation process at the RNA and protein levels using real-time PCR, western blotting, immunofluorescence and flow cytometry. As apoptotic cells can take up exogenous insulin from the culture medium, we measured both *INS* mRNA as well as C-peptide and proinsulin protein to demonstrate *de novo* synthesis of insulin[12–14]. We also used electron microscopy to image β-secretory granules within the cell.

Stage 1 of our protocol involves formation of DE[24]. We reported previously that the efficiency of DE production increases as serum supplementation is decreased[24]. We discovered that elevated phosphoinositol 3-kinase (PI-3-kinase) signaling, resulting from the presence of IGF in serum or of insulin in serum-free medium, inhibits the differentiation of hES cells to DE[49]. PI-3-kinase signaling is required to maintain hES cells in a self-renewing state. Thus, it is important to remove self-renewal signals during the initial stage of hES cell differentiation. For these reasons, we initiate hES cell differentiation using a brief PBS wash to remove the high levels of recombinant insulin present in KnockOut serum replacement. Starting cultures are >75% confluent and incubated in RPMI medium containing 100 ng/ml activin A supplemented with 0, 0.2% and 0.2% (vol/vol) FBS on days 1–3, respectively. For many cell lines, addition of Wnt3a at 25 ng/ml on day 1 will improve transition through the mesendoderm state.

We believe that another important issue for efficient endoderm differentiation of hES cells is avoidance of embryoid body formation, as this may hinder uniform exposure of cells on the interior of the aggregates to medium and factors. The combined effect of reduced PI-3-kinase signaling and use of a two-dimensional culture environment results in both rapid and synchronous induction of hES cell differentiation, which is critical for orchestrating efficient transitions through subsequent stages of differentiation.

During stage 2, DE differentiates towards endoderm of the primitive gut tube, as demonstrated by downregulation of *CER* and upregulation of *HNF1B* and *HNF4A*. The use of KAAD-cyclopamine at this step is consistent with the known importance of hedgehog-signaling inhibition during early pancreas development[18]. We also use FGF10, a factor involved in proliferation of pancreatic epithelium[21,50,51] and perhaps in endoderm patterning[52].

In stage 3, KAAD-cyclopamine and FGF10 are maintained and RA, which is required for pancreatic organogenesis[17], is added. This results in a large increase in expression of *HNF6*, *HLXB9* and *PDX1*, all of which are expressed in the posterior foregut and are required for pancreas development[53–56].

During stage 4, after removal of RA, two closely associated intermediates arise: pancreatic epithelial progenitors and endocrine precursors. As in the embryo, the pancreatic endoderm is demarcated in our cultures by large regions of cells that show overlapping expression of *PDX1* and *NKX6-1*. In the embryo, *NGN3* is expressed in endocrine progenitors[19,57,58]. NGN3-expressing cells are detected in our cultures within the domains of PDX1/NKX6-1 cells, and many of them coexpress NKX2-2. Also, at stage 4 there is a substantial increase in expression of *NGN3* and its downstream target gene *PAX4*. Expression of *NGN3* and *PAX4* decreases during stage 5, consistent with the transient expression of these genes *in vivo*. As *Ngn3* expression in the pancreas occurs as a result of decreased Notch signaling, our initial protocols included the Notch-pathway inhibitor DAPT. However, further studies showed that although DAPT may have a slight beneficial effect, it is not required for *NGN3* expression during stage 4. Thus, an unknown mechanism inherent to the culture system upregulates *NGN3* expression specifically in stage 4. To our knowledge, production of these transient endocrine precursors from ES cells has not been reported previously.

During stage 5, after ~2 weeks of differentiation, hormone-expressing cells appear. Several days later, hormone expression becomes more intense and cells expressing each of the five pancreatic endocrine hormones are detected. Many cells express more than one hormone. Ghrelin, however, is rarely coexpressed with another hormone, which may indicate that some proportion of the ghrelin-expressing cells are derived from the intestinal lineage. Polyhormonal cells have been described during the primary transition stage of early fetal development in both rodents[59] and humans[60,61]. In the mouse, direct lineage tracing via genetic manipulations has revealed that mature α- and β-cells

arise from independent lineages that never coexpressed glucagon and insulin[62]. Whether this aspect of mouse development is conserved in humans is unknown.

It is possible that our hES cell–derived hormone coexpressing cells are analogous to the endocrine cells of the primary transition. However, several aspects of our differentiation process are characteristic of the secondary transition. For example, substantial numbers of cells expressing SST, PPY and amylase are produced[63], and insulin-immunoreactive cells appear before and in greater numbers than glucagon-immunoreactive cells[64]. Alternatively, polyhormonal expression may result from a failure of our differentiation protocol to maintain the appropriate transcription factor code. For instance, although some of the NKX2-2–expressing endocrine progenitors initially coexpress NKX6-1, expression of NKX6-1 does not persist in insulin-expressing cells as would be expected (**Fig. 3a**,**c** and data not shown). In this regard, it is interesting to note that a consequence of inhibiting *NKX6-1* expression in an insulinoma cell line is aberrant upregulation of glucagon expression[65]. Along similar lines, PDX1 expression is maintained in our insulin-expressing cells for ~5 d after initial expression of insulin, but then gradually declines (**Fig. 3e** and data not shown).

These observations are important in light of our attempts to mature the insulin-expressing cells to a glucose-responsive state. In mice, the maturation of insulin-expressing cells formed during the secondary transition is characterized by a switch from MafB$^+$MafA$^-$ to MafB$^-$MafA$^+$ status[66]. This switch occurs in cells that already express Nkx6-1 and is preceded by an increase in Pdx1 expression. Our hES cell–derived insulin-expressing cells coexpress MAFB similarly to the insulin-expressing cells of the 13.5-week fetal human pancreas (**Supplementary Fig. 8** online). Although we were unable to characterize the expression of MAFA in these cells or in human pancreas sections owing to a lack of suitable human immunoreactive antibodies, we speculate that our hES cell–derived cells have not made the switch from MAFB$^+$MAFA$^-$ to MAFB$^-$MAFA$^+$, given that expression of NKX6-1 and PDX1 is not maintained.

We have focused on characterizing the insulin-expressing endocrine cells because this cell type is most critical for developing a diabetes cell therapy. The insulin content of the hES cell–derived dithizone-stained cell clusters ranged from 14 to 208 pmol/μg DNA. This exceeds the 2 pmol/μg DNA reported for fetal human islet cell clusters[67,68] and is in the same range as the insulin content of primary adult human islets, which ranged from 58-310 pmol/μg DNA. To our knowledge, no previous study has reported such a high insulin content in a cell derived from an ES cell. However, our hES cell–derived cells process proinsulin less efficiently than adult islets, which process 97% of their proinsulin content. Nonetheless, C-peptide in the hES cell–derived cells is consistently secreted in a regulated manner, with rapid release kinetics in response to both pharmacological modulators and metabolic stimulators. In addition, we demonstrate by electron microscopy that the endocrine cells contain numerous secretory granules.

These findings indicate that the hES cell–derived insulin-expressing cells contain many cell components critical to β-cell function. However, C-peptide secretion in our cultures was only minimally responsive to

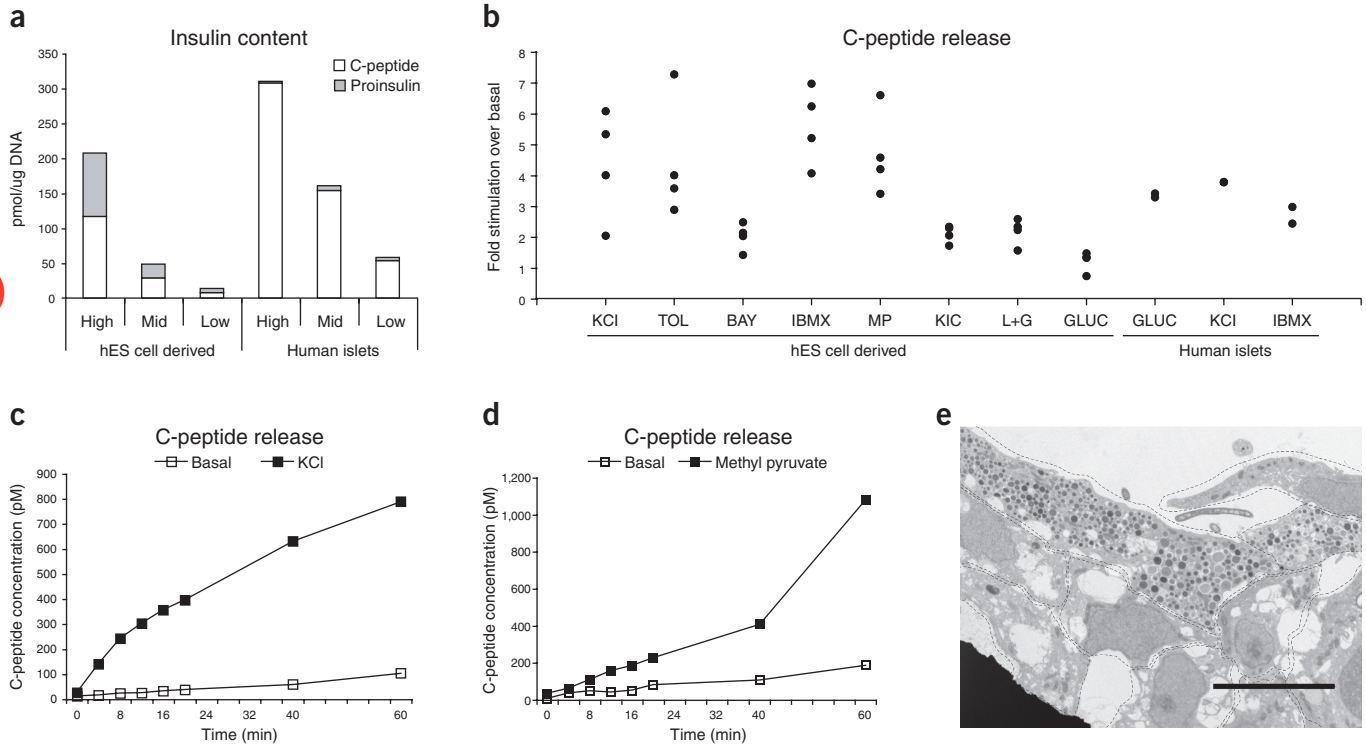

Figure 6 High insulin content and robust C-peptide release. (**a**) Clusters of hES cell–derived endocrine cells isolated using DTZ have a range of total insulin content (sum of C-peptide + proinsulin) that overlaps that observed for primary adult human islets. (**b**) Fold stimulation of C-peptide release over the respective basal condition for multiple pharmacological as well as nutrient secretagogues. TOL, tolbutamide; BAY, (–)-BAY K8644; MP, methylpyruvate; L+G, L-leucine plus L-glutamine. (**c**,**d**) The C-peptide release in response to KCl and methylpyruvate shows rapid kinetics. (**e**) Electron micrograph of hES cell–derived endocrine cells showing two cells that contain numerous secretory granules. Although a mixture of granule morphologies seems to be present in most cells, some granules show a clear halo surrounding a less dense core, a morphology that is characteristic of an insulin-containing granule. Cell boundaries are outlined. Scale bar, 10 μm.

glucose. As the fetal pancreas also responds to multiple secretory stimuli but not to glucose, we conclude that the insulin-expressing cells we have generated may be similar to immature fetal β-cells. Future research will focus on defining conditions that further differentiate the endocrine hormone–expressing cells to mature pancreatic islet cells. Of interest in this regard are data showing that human fetal islets require 12–16 weeks to achieve glucose-stimulated insulin release after kidney capsule transplantation[69].

Assessment by flow cytometry of the quantity of insulin-producing cells showed that our cultures produce an average of 7% and as many as 12% insulin-positive cells. Although some hES cells die during the transition to mesendoderm, the differentiation protocol maintains stable numbers of cells from stage 1 and beyond. A 60-mm plate with 10 million undifferentiated human ES cells yields ~10 million cells at stage 5, of which 7%, on average, are insulin-expressing cells. Suboptimal differentiation to DE (activin A 30 ng/ml during stage 1) results in only 0.3% insulin-positive cells. Moreover, cells differentiated to either the neural or extraembryonic lineages rather than toward DE during stage 1 express extremely low levels of insulin (>100,000-fold lower) and low levels of markers of pancreatic endodermal intermediates.

Regarding the various hES cell lines we assessed, we speculate that their varying endocrine differentiation efficiencies may result from intrinsic differences in the way the cells respond to the culture milieu as well as the distinctive environments they generate. For example, consistent with *in vivo* pancreatic development, it is possible that other cell types within our cultures, such as mesoderm, contribute to differentiation of the hES cells. For instance, under the conditions described here, different hES cell lines may initially generate different proportions of mesoderm and endoderm. This ratio may affect the efficiency of differentiation to endocrine cells.

An interesting issue to address in future studies is whether our differentiation process occurs via an inductive or a selective mechanism; discriminating between these two possibilities will require assessment of cell proliferation and death throughout the course of differentiation. However, an inductive mechanism is suggested by the observation that a considerable proportion of the cells in the population transition through each of the endoderm intermediates with rapid kinetics and a limited degree of cell death, as evidenced by the minimal cell debris in the cultures.

In sum, we have demonstrated that hES cells can be efficiently differentiated to hormone-expressing endocrine cells through a series of endodermal intermediates that are similar to those that occur *in vivo*. We are awed by the capacity of hES cells to recapitulate development *ex vivo* and are optimistic that these unique cells will ultimately represent a renewable source of pancreatic β-cells for people with diabetes.

METHODS

Cell culture. Undifferentiated hES cells were maintained on mouse embryo fibroblast feeder layers (Specialty Media) in DMEM/F12 (Mediatech) supplemented with 20% (vol/vol) KnockOut serum replacement (Invitrogen), 1 mM nonessential amino acids (Invitrogen), Glutamax (Invitrogen), penicillin/streptomycin (Invitrogen), 0.55 mM 2-mercaptoethanol (Invitrogen), 4 ng/ml recombinant human FGF2 (R&D Systems) and 10–25 ng/ml activin A (R&D Systems). Cultures were manually passaged at a 1:4–1:8 split ratio every 5–7 d. Differentiation was carried out as indicated in **Figure 1** in RPMI (Mediatech), DMEM (HyClone) or CMRL (Invitrogen) media as indicated, each supplemented with Glutamax, penicillin/streptomycin, and varying concentrations of defined FBS (HyClone) or 1% (vol/vol) B27 supplement (Invitrogen) where indicated. On occasion, stages 3 and 4 were carried out in CMRL with 1% (vol/vol) B27 supplement. The use of DAPT and exendin-4 during stage 4, as well as the use of exendin-4, IGF-1 and HGF during stage 5, were routinely included in the procedure, but we have observed only minor differences in the differentiation when they are omitted. Before differentiation was initiated, hES cells were given a brief wash in PBS with Ca^{2+} and Mg^{2+} (Mediatech). Recombinant human activin A (100 ng/ml), mouse Wnt3a (25 ng/ml), human FGF10 (50 ng/ml), human noggin (50 ng/ml), human follistatin (100 ng/ml) and human BMP4 (100 ng/ml) were purchased from R&D Systems. KAAD-cyclopamine (0.25 μM) was purchased from Toronto Research Chemicals, all-*trans* retinoic acid (2 μM), DAPT (1 μM), exendin 4 (50 ng/ml) and IGF-1 (50 ng/ml) were from Sigma, and HGF (50 ng/ml) was from Peprotech. SU5402 (3 μM) was a gift (see Acknowledgments). With the exception of the data presented in **Supplementary Figure 7**, all of the data were generated using the CyT203 hES cell line. In addition, the differentiation experiments were repeated three or more times with similar results.

Western blot analyses. ES cell–derived cultures on 60-mm plates were harvested into 200 μl of 1× lysis solution (50 mM Tris, pH 8.0, 150 mM NaCl, 1% (wt/vol) Triton X-100, 0.1% (wt/vol) SDS, 1% (wt/vol) deoxycholate) supplemented with a cocktail of protease inhibitors (Roche). Electrophoresis of 15-μl lysates on polyacrylamide gels (4–12% (wt/vol) Bis-Tris NuPage, Invitrogen) was followed by electroblotting onto PDVF membranes (Bio-Rad) and detection using horseradish peroxidase–conjugated secondary antibodies (Jackson ImmunoResearch Laboratories) and chemiluminescent (SuperSignal West Pico, Pierce) exposure of BioMax film (Kodak). The following concentrations were used for primary antibodies: goat antibody to Oct4/POU5F1 (anti-Oct/POU5FI; Santa Cruz Biotechnology, sc-9081), 1 μg/ml; rat anti-SOX17 (Genovac), 1:1,000; goat anti-FOXA2/HNF3β (R&D Systems, AF2400), 0.2 μg/ml goat anti-HNF1B (R&D Systems, AF3330), 0.4 μg/ml; rabbit anti-PDX1 (Chemicon, AB3243), 1:2,500; mouse anti-NKX2-2 (Developmental Studies Studies Hybridoma Bank, 74.5A5), 20 μg/ml; mouse anti-NKX6-1 (Developmental Studies Studies Hybridoma Bank, F55A12 and F65A2), 10 μg/ml; rabbit anti-PAX6 (Chemicon, AB5409), 2 μg/ml, rabbit anti-C-peptide (Linco, 4020-01; also detects proinsulin), 1:200; mouse anti-GAPDH (Chemicon, MAB374), 2 μg/ml.

Immunofluorescence. Cultures were fixed for 15 min at 24 °C in 4% (wt/vol) paraformaldehyde in PBS, washed several times in PBS and blocked for 30 min in PBST (PBS/0.1% (wt/vol) Triton X-100 (Sigma)) containing 5% (vol/vol) normal donkey serum (nds, Jackson ImmunoResearch Laboratories). Primary and secondary antibodies were diluted in PBST/5% nds. Primaries were incubated for 24 h at 4 °C or 2 h at 24 °C, and secondary antibodies were incubated for 1 h at 24 °C. These buffers were modified in the case of PDX1 stainings: the blocking step included 50 mM glycine, 2% BSA and only 2% nds, and the incubation buffer omitted Triton. The following antibodies and dilutions were used: rat anti-SOX17, 1:500 (ref. 24); goat anti-HNF1B, 1:100 (Santa Cruz Biotechnology, SC-7411); rabbit anti-PDX1, 1:750 (Chemicon, AB3243); rabbit anti-HNF6, 1:100 (Santa Cruz Biotechnology, SC-13050); rabbit anti-HN4a, 1:300 (Santa Cruz Biotechnology, SC-8987); mouse anti-NKX2-2, 1:10 (Developmental Studies Studies Hybridoma Bank, 74.5A5); mouse anti-NKX6-1 (F55A12) and rabbit anti-NKX6-1, 1:1,200 (gifts; see Acknowledgments); rabbit anti-NGN3, 1:2,000 (gift; see Acknowledgments), goat anti-NEURO-D, 1:100 (Santa Cruz Biotechnology, SC-1084); mouse anti-ISL1/2, 1:20 (Developmental Studies Hybridoma Bank, 39.4D5); rabbit anti-PAX6, 1:1,000 (Chemicon, AB5409), guinea pig anti-insulin,1:500 (Dako, A0564); rabbit anti-C-peptide, 1:500 (Linco, 4020-01; note that this antibody detects both C-peptide and proinsulin); mouse anti-proinsulin, 1:500 (Abcam, ab8301-100); mouse anti-glucagon, 1:500 (Sigma, G2654); rabbit anti-somatostatin, 1:300 (Dako, A0566); mouse anti-PP, 1:300 (Dako, A0169); goat anti-ghrelin, 1:300 (Santa Cruz Biotechnology, sc10368); rabbit anti-synaptophysin, 1:200 (Dako, A0010); rabbit anti-IAPP, 1:300 (Fitzgerald, RDI-PRO16002); rabbit anti-amylase, 1:500 (Sigma, A8273). Cy3- and Cy5-conjugated donkey antibodies against mouse, rabbit and guinea pig were used at 1:500 (Jackson ImmunoResearch Laboratories). Alexa-488– and Alexa-555–conjugated donkey antibodies against mouse, rat, rabbit, guinea pig and goat (Molecular Probes) were used at 1:500 dilution.

Electron microscopy. On some areas of the culture dish, hES cell–derived endocrine cells clump together and have a distinct morphology, allowing their dissection with fine tungsten needles. For conventional electron microscopy (EM), these dissected clumps of cells were fixed in 100 mM cacodylate buffer, pH 7.4,

containing 3% wt/vol formaldehyde, 1.5% (wt/vol) glutaraldehyde and 2.5% (wt/vol) sucrose for 1 h, washed and osmicated at 4 °C in Palade's fixative containing 1% (vol/vol) OsO_4. Cells were then washed, treated with tannic acid, stained with uranyl acetate, dehydrated through a graded series of ethanol solutions and embedded in epon. 80-nm sections were cut on a LEICA UCT ultramicrotome and analyzed on a Philips 420 TEM at 80 kV.

C-peptide content and release assays. Research-grade primary adult human islets were isolated and cultured according to procedures that have been optimized for use in human clinical trials (ADA abstract # 63-LB; 2006). C-peptide or proinsulin levels in culture supernatants or cell lysates were measured using the ultrasensitive C-peptide ELISA or proinsulin ELISA (Alpco Diagnostics). For total C-peptide content analysis, hES cell cultures differentiated to endocrine cell stage were stained with dithizone (Sigma) and dithizone-positive areas were selected and then sonicated in 100 µl of water. DNA content was measured using PicoGreen (Invitrogen). C-peptide release was measured by incubating either hES cell cultures or 20–30 adult human islets in Krebs-Ringer solution with bicarbonate and HEPES (KRBH; 129 mM NaCl, 4.8 mM KCl, 2.5 mM $CaCl_2$, 1.2 mM KH_2PO_4, 1.2 mM $MgSO_4$, 5 mM $NaHCO_3$, 10 mM HEPES, 0.1% (wt/vol) BSA). An initial 1-h incubation was considered a wash; the medium was discarded and this was followed by a 1-h incubation in basal medium containing 2 mM D-glucose with 18 mM L-glucose and then a 1-h incubation in the stimulation condition (20 mM D-glucose, 0.5 mM IBMX, 100 µM tolbutamide, 30 mM KCl, 10 mM each L-glutamine and L-leucine, 10 mM ketoisocaproic acid, 2 µM (–)-BAY K8644 and 15 mM methylpyruvate (all purchased from Sigma)). The fold stimulation was calculated for each culture by dividing the C-peptide concentration in the stimulation supernatant by the C-peptide concentration in the basal supernatant. To determine the kinetics of C-peptide release, plates were incubated on a rotating shaker and the supernatant was sampled at the indicated times.

Real-time quantitative PCR. Small scrapings of cells were harvested from differentiating plates, and total RNA was isolated from duplicate or triplicate samples with a 6100 nucleic acid extractor (Applied Biosystems) and 100–500 ng used for reverse transcription with iScript cDNA synthesis kit (Bio-Rad). PCR reactions were run in duplicate using $1/40^{th}$ of the cDNA per reaction and 400 nM forward and reverse primers with QuantiTect SYBR Green master mix (Qiagen). Alternatively, QuantiTect Primer Assays (Qiagen) were used according to the manufacturers instructions. Real-time PCR was performed using the Rotor Gene 3000 (Corbett Research). Relative quantification was performed in relation to a standard curve. The standard curve was created using a mixture of total RNA samples from various fetal human endoderm tissues and differentiated hES cells, and 1 µg was used per cDNA reaction in creating the standard curve. Quantified values for each gene of interest were normalized against the input determined by two housekeeping genes (*CYCG* and *GUSB* or *TBP*). After normalization, the samples were plotted relative to the lowest detectable sample in the dataset and the standard deviation of the four- or six-gene expression measurements was reported. Primer sequences are reported in **Supplementary Table 1** online. Total RNA from adult human pancreas was from Ambion (cat. no. 7954) and 20-week fetal pancreas from BioChain.

Flow cytometry. Single-cell suspensions of differentiating hES cell cultures were obtained by dissociating cells with either TrypLE (Invitrogen #12563-011) or Accutase (Innovative Cell Technologies #AT104) at 37 °C. Intracellular antibody staining was performed using Becton Dickinson Cytofix/Cytoperm and Becton Dickinson Perm/Wash buffer according to manufacturer instructions. The following concentrations of primary and secondary antibodies were used: guinea pig anti-insulin, 1:1,000 (DakoCytomation #A0564), rabbit anti-synaptophysin, 1:100 (DakoCytomation #A0010), donkey anti-guinea pig–Cy5, 1:1,000 (Jackson ImmunoResearch Laboratories #706-176-148) and donkey anti-rabbit–Alexa 488, 1:2,000 (Invitrogen #A21206). Flow cytometry data were acquired on a Becton Dickinson FACSAria and analyzed using Becton Dickinson FACSDiva software.

Note: Supplementary information is available on the Nature Biotechnology website.

ACKNOWLEDGMENTS

We thank Matthias Hebrok, Mike German and Alberto Hayek for critical review of the manuscript; Alberto Hayek for total RNA from 11- and 14-week fetal human pancreas; and Michael McCaffery at John Hopkins University for performing the EM analyses. SU5402 was a gift from A. Terskikh, mouse anti-NKX6-1 (F55A12) and rabbit anti-NKX6-1 were gifts from Ole Madsen, and rabbit anti-NGN3 was a gift from Mike German. The CyT203 and CyT49 cell lines were derived with partial funding from the Juvenile Diabetes Research Foundation.

COMPETING FINANCIAL INTERESTS

The authors declare that they have no competing financial interests.

Published online at http://www.nature.com/naturebiotechnology/
Reprints and permissions information is available online at http://npg.nature.com/reprintsandpermissions/

1. Hoffman, L.M. & Carpenter, M.K. Characterization and culture of human embryonic stem cells. *Nat. Biotechnol.* **23**, 699–708 (2005).
2. Liew, C.G. *et al.* Human embryonic stem cells: possibilities for human cell transplantation. *Ann. Med.* **37**, 521–532 (2005).
3. Bonner-Weir, S. & Weir, G.C. New sources of pancreatic beta-cells. *Nat. Biotechnol.* **23**, 857–861 (2005).
4. Madsen, O.D. Stem cells and diabetes treatment. *APMIS* **113**, 858–875 (2005).
5. Assady, S. *et al.* Insulin production by human embryonic stem cells. *Diabetes* **50**, 1691–1697 (2001).
6. Segev, H., Fishman, B., Ziskind, A., Shulman, M. & Itskovitz-Eldor, J. Differentiation of human embryonic stem cells into insulin-producing clusters. *Stem Cells* **22**, 265–274 (2004).
7. Baharvand, H., Jafary, H., Massumi, M. & Ashtiani, S.K. Generation of insulin-secreting cells from human embryonic stem cells. *Dev. Growth Differ.* **48**, 323–332 (2006).
8. Xu, X. *et al.* Endoderm and pancreatic islet lineage differentiation from human embryonic stem cells. *Cloning Stem Cells* **8**, 96–107 (2006).
9. Kwon, Y.D. *et al.* Cellular manipulation of human embryonic stem cells by TAT-PDX1 protein transduction. *Mol. Ther.* **12**, 28–32 (2005).
10. Hori, Y., Gu, X., Xie, X. & Kim, S.K. Differentiation of insulin-producing cells from human neural progenitor cells. *PLoS Med.* **2**, e103 (2005).
11. Roche, E., Sepulcre, P., Reig, J.A., Santana, A. & Soria, B. Ectodermal commitment of insulin-producing cells derived from mouse embryonic stem cells. *FASEB J.* **19**, 1341–1343 (2005).
12. Sipione, S., Eshpeter, A., Lyon, J.G., Korbutt, G.S. & Bleackley, R.C. Insulin expressing cells from differentiated embryonic stem cells are not beta cells. *Diabetologia* **47**, 499–508 (2004).
13. Rajagopal, J., Anderson, W.J., Kume, S., Martinez, O.I. & Melton, D.A. Insulin staining of ES cell progeny from insulin uptake. *Science* **299**, 363 (2003).
14. Hansson, M. *et al.* Artifactual insulin release from differentiated embryonic stem cells. *Diabetes* **53**, 2603–2609 (2004).
15. Tam, P.P., Williams, E.A. & Chan, W.Y. Gastrulation in the mouse embryo: ultrastructural and molecular aspects of germ layer morphogenesis. *Microsc. Res. Tech.* **26**, 301–328 (1993).
16. Wells, J.M. & Melton, D.A. Vertebrate endoderm development. *Annu. Rev. Cell Dev. Biol.* **15**, 393–410 (1999).
17. Stafford, D., Hornbruch, A., Mueller, P.R. & Prince, V.E. A conserved role for retinoid signaling in vertebrate pancreas development. *Dev. Genes Evol.* **214**, 432–441 (2004).
18. Lau, J., Kawahira, H. & Hebrok, M. Hedgehog signaling in pancreas development and disease. *Cell. Mol. Life Sci.* **63**, 642–652 (2006).
19. Gu, G., Dubauskaite, J. & Melton, D.A. Direct evidence for the pancreatic lineage: $NGN3^+$ cells are islet progenitors and are distinct from duct progenitors. *Development* **129**, 2447–2457 (2002).
20. Wilson, M.E., Scheel, D. & German, M.S. Gene expression cascades in pancreatic development. *Mech. Dev.* **120**, 65–80 (2003).
21. Bhushan, A. *et al.* Fgf10 is essential for maintaining the proliferative capacity of epithelial progenitor cells during early pancreatic organogenesis. *Development* **128**, 5109–5117 (2001).
22. Murtaugh, L.C. & Melton, D.A. Genes, signals, and lineages in pancreas development. *Annu. Rev. Cell Dev. Biol.* **19**, 71–89 (2003).
23. Jensen, J. Gene regulatory factors in pancreatic development. *Dev. Dyn.* **229**, 176–200 (2004).
24. D'Amour, K.A. *et al.* Efficient differentiation of human embryonic stem cells to definitive endoderm. *Nat. Biotechnol.* **23**, 1534–1541 (2005).
25. Yamaguchi, T.P. Heads or tails: Wnts and anterior-posterior patterning. *Curr. Biol.* **11**, R713–R724 (2001).
26. Kanai-Azuma, M. *et al.* Depletion of definitive gut endoderm in Sox17-null mutant mice. *Development* **129**, 2367–2379 (2002).
27. Yasunaga, M. *et al.* Induction and monitoring of definitive and visceral endoderm differentiation of mouse ES cells. *Nat. Biotechnol.* **23**, 1542–1550 (2005).
28. McGrath, K.E., Koniski, A.D., Maltby, K.M., McGann, J.K. & Palis, J. Embryonic expression and function of the chemokine SDF-1 and its receptor, CXCR4. *Dev. Biol.* **213**, 442–456 (1999).
29. Sasaki, H. & Hogan, B.L. Differential expression of multiple fork head related genes during gastrulation and axial pattern formation in the mouse embryo. *Development* **118**, 47–59 (1993).
30. Biben, C. *et al.* Murine cerberus homologue mCer-1: a candidate anterior patterning molecule. *Dev. Biol.* **194**, 135–151 (1998).

31. Barbacci, E. *et al.* Variant hepatocyte nuclear factor 1 is required for visceral endoderm specification. *Development* **126**, 4795–4805 (1999).
32. Coffinier, C., Barra, J., Babinet, C. & Yaniv, M. Expression of the vHNF1/HNF1β homeoprotein gene during mouse organogenesis. *Mech. Dev.* **89**, 211–213 (1999).
33. Duncan, S.A. *et al.* Expression of transcription factor HNF-4 in the extraembryonic endoderm, gut, and nephrogenic tissue of the developing mouse embryo: HNF-4 is a marker for primary endoderm in the implanting blastocyst. *Proc. Natl. Acad. Sci. USA* **91**, 7598–7602 (1994).
34. Sun, Z. & Hopkins, N. vhnf1, the MODY5 and familial GCKD-associated gene, regulates regional specification of the zebrafish gut, pronephros, and hindbrain. *Genes Dev.* **15**, 3217–3229 (2001).
35. Chen, Y. *et al.* Retinoic acid signaling is essential for pancreas development and promotes endocrine at the expense of exocrine cell differentiation in *Xenopus*. *Dev. Biol.* **271**, 144–160 (2004).
36. Stafford, D. & Prince, V.E. Retinoic acid signaling is required for a critical early step in zebrafish pancreatic development. *Curr. Biol.* **12**, 1215–1220 (2002).
37. Molotkov, A., Molotkova, N. & Duester, G. Retinoic acid generated by Raldh2 in mesoderm is required for mouse dorsal endodermal pancreas development. *Dev. Dyn.* **232**, 950–957 (2005).
38. Martin, M. *et al.* Dorsal pancreas agenesis in retinoic acid-deficient Raldh2 mutant mice. *Dev. Biol.* **284**, 399–411 (2005).
39. Hebrok, M., Kim, S.K. & Melton, D.A. Notochord repression of endodermal Sonic hedgehog permits pancreas development. *Genes Dev.* **12**, 1705–1713 (1998).
40. Rindi, G., Leiter, A.B., Kopin, A.S., Bordi, C. & Solcia, E. The "normal" endocrine cell of the gut: changing concepts and new evidences. *Ann. NY Acad. Sci.* **1014**, 1–12 (2004).
41. Tomita, T. New markers for pancreatic islets and islet cell tumors. *Pathol. Int.* **52**, 425–432 (2002).
42. Latif, Z.A., Noel, J. & Alejandro, R. A simple method of staining fresh and cultured islets. *Transplantation* **45**, 827–830 (1988).
43. Frederickson, C. Imaging zinc: old and new tools. *Sci. STKE* **2003**, pe18 (2003).
44. Sturgess, N.C., Ashford, M.L., Cook, D.L. & Hales, C.N. The sulphonylurea receptor may be an ATP-sensitive potassium channel. *Lancet* **2**, 474–475 (1985).
45. Misler, S. *et al.* Stimulus-secretion coupling in beta-cells of transplantable human islets of Langerhans. Evidence for a critical role for Ca^{2+} entry. *Diabetes* **41**, 662–670 (1992).
46. Pyne, N.J. & Furman, B.L. Cyclic nucleotide phosphodiesterases in pancreatic islets. *Diabetologia* **46**, 1179–1189 (2003).
47. Prentki, M. & Matschinsky, F.M. Ca^{2+}, cAMP, and phospholipid-derived messengers in coupling mechanisms of insulin secretion. *Physiol. Rev.* **67**, 1185–1248 (1987).
48. Klimstra, D.S. Pancreas. in *Histology for Pathologists* (ed. Sternberg, S.S.) 613–647 (Lippincott-Raven Publishers, Philadelphia, 1997).
49. McLean, A.B. *et al.* Activin A efficiently specifies definitive endoderm from human embryonic stem cells only when PI3K signaling is suppressed. *Stem Cells* (in the press).
50. Hart, A., Papadopoulou, S. & Edlund, H. Fgf10 maintains notch activation, stimulates proliferation, and blocks differentiation of pancreatic epithelial cells. *Dev. Dyn.* **228**, 185–193 (2003).
51. Ye, F., Duvillie, B. & Scharfmann, R. Fibroblast growth factors 7 and 10 are expressed in the human embryonic pancreatic mesenchyme and promote the proliferation of embryonic pancreatic epithelial cells. *Diabetologia* **48**, 277–281 (2005).
52. Jacquemin, P. *et al.* An endothelial-mesenchymal relay pathway regulates early phases of pancreas development. *Dev. Biol.* **290**, 189–199 (2006).
53. Jonsson, J., Carlsson, L., Edlund, T. & Edlund, H. Insulin-promoter-factor 1 is required for pancreas development in mice. *Nature* **371**, 606–609 (1994).
54. Jacquemin, P., Lemaigre, F.P. & Rousseau, G.G. The Onecut transcription factor HNF-6 (OC-1) is required for timely specification of the pancreas and acts upstream of Pdx-1 in the specification cascade. *Dev. Biol.* **258**, 105–116 (2003).
55. Harrison, K.A., Thaler, J., Pfaff, S.L., Gu, H. & Kehrl, J.H. Pancreas dorsal lobe agenesis and abnormal islets of Langerhans in *Hlxb9*-deficient mice. *Nat. Genet.* **23**, 71–75 (1999).
56. Li, H., Arber, S., Jessell, T.M. & Edlund, H. Selective agenesis of the dorsal pancreas in mice lacking homeobox gene *Hlxb9*. *Nat. Genet.* **23**, 67–70 (1999).
57. Schwitzgebel, V.M. *et al.* Expression of neurogenin3 reveals an islet cell precursor population in the pancreas. *Development* **127**, 3533–3542 (2000).
58. Gradwohl, G., Dierich, A., LeMeur, M. & Guillemot, F. neurogenin3 is required for the development of the four endocrine cell lineages of the pancreas. *Proc. Natl. Acad. Sci. USA* **97**, 1607–1611 (2000).
59. Teitelman, G., Alpert, S., Polak, J.M., Martinez, A. & Hanahan, D. Precursor cells of mouse endocrine pancreas coexpress insulin, glucagon and the neuronal proteins tyrosine hydroxylase and neuropeptide Y, but not pancreatic polypeptide. *Development* **118**, 1031–1039 (1993).
60. Polak, M., Bouchareb-Banaei, L., Scharfmann, R. & Czernichow, P. Early pattern of differentiation in the human pancreas. *Diabetes* **49**, 225–232 (2000).
61. De Krijger, R.R. *et al.* The midgestational human fetal pancreas contains cells coexpressing islet hormones. *Dev. Biol.* **153**, 368–375 (1992).
62. Herrera, P.L., Nepote, V. & Delacour, A. Pancreatic cell lineage analyses in mice. *Endocrine* **19**, 267–278 (2002).
63. Slack, J.M. Developmental biology of the pancreas. *Development* **121**, 1569–1580 (1995).
64. Pictet, R.L. & Rutter, W.J. Development of the embryonic endocrine pancreas. in *Handbook of Physiology* (eds. Steiner, D.F. & Frenkel, N.) 25–66 (Williams and Wilkins, Washington, DC, 1972).
65. Schisler, J.C. *et al.* The Nkx6.1 homeodomain transcription factor suppresses glucagon expression and regulates glucose-stimulated insulin secretion in islet beta cells. *Proc. Natl. Acad. Sci. USA* **102**, 7297–7302 (2005).
66. Nishimura, W. *et al.* A switch from MafB to MafA expression accompanies differentiation to pancreatic beta-cells. *Dev. Biol.* **293**, 526–539 (2006).
67. Demeterco, C., Beattie, G.M., Dib, S.A., Lopez, A.D. & Hayek, A. A role for activin A and betacellulin in human fetal pancreatic cell differentiation and growth. *J. Clin. Endocrinol. Metab.* **85**, 3892–3897 (2000).
68. Hayek, A. & Beattie, G.M. Experimental transplantation of human fetal and adult pancreatic islets. *J. Clin. Endocrinol. Metab.* **82**, 2471–2475 (1997).
69. Beattie, G.M., Butler, C. & Hayek, A. Morphology and function of cultured human fetal pancreatic cells transplanted into athymic mice: a longitudinal study. *Cell Transplant.* **3**, 421–425 (1994).
70. Kanai, Y. *et al.* Identification of two Sox17 messenger RNA isoforms, with and without the high mobility group box region, and their differential expression in mouse spermatogenesis. *J. Cell Biol.* **133**, 667–681 (1996).